J Appl Electrochem (2009) 39:1305–1311
DOI 10.1007/s10800-009-9803-8

ORIGINAL PAPER

Effect of SiC and Al_2O_3 particles on the electrodeposition of Zn, Co and ZnCo: II. Electrodeposition in the presence of SiC and Al_2O_3 and production of ZnCo–SiC and ZnCo–Al_2O_3 coatings

Paulo C. Tulio · Ivani A. Carlos

Received: 14 February 2008 / Accepted: 13 January 2009 / Published online: 31 January 2009

Abstract SiC or Al_2O_3 microsized particles were added to acid sulfate-based solutions for the electrodeposition of Zn, Co, and ZnCo. Initially, their effects on the electrochemical processes were evaluated. The Zn electrodeposition rate was increased in both SiC and Al_2O_3-loaded solutions. The Co electrodeposition rate was also increased by SiC. However, Al_2O_3 decreased it, especially at the beginning. Both SiC and Al_2O_3 influenced the electrodeposition of ZnCo positively at moderate loadings. The factors involved in producing ZnCo–SiC and ZnCo–Al_2O_3 composites were evaluated. ZnCo–SiC composites could be deposited with a higher [Co/Zn] ratio in the metal matrix than for pure ZnCo. In ZnCo–Al_2O_3, the [Co/Zn] ratio was smaller than in ZnCo and ZnCo–SiC. It was necessary to reduce the $CoSO_4$ concentration to improve the Al_2O_3 co-deposition. The variation in [Co/Zn] ratio could, in principle, be related to the effects of SiC and Al_2O_3 on the individual Zn and Co electrodeposition.

Keywords Zn, Co, and ZnCo · Electrodeposition · Acidic media · Composites · ZnCo–SiC and ZnCo–Al_2O_3

1 Introduction

In Part I of this study [1], the electrochemical features of Zn, Co and ZnCo electrodeposition on steel from particle-free acid sulfate solutions were investigated. In this Part II, SiC or Al_2O_3 micro particles were added to the electrodeposition solutions and their effects on the electrodeposition processes and the ZnCo–SiC and ZnCo–Al_2O_3 deposits were assessed.

There have been fewer reports on metal alloy composite coatings produced by electrodeposition than on single-metal deposits. The additional complications in alloy electrodeposition, compared to the single-metal case, make these systems less suitable for the investigation of particle co-deposition mechanisms.

However, electrocomposite alloy coatings exhibit some interesting features. For example, Wu et al. [2, 3] studied the co-deposition of α-Al_2O_3 (mean diameter (ϕ) 0.5 μm) with CoNi alloys in sulfamate solutions. They found that the Al_2O_3 in suspension polarizes the reduction process and causes the Co content in the alloy to be increased. Muller et al. [4] studied the co-deposition of α-SiC ($\phi = 7$ μm) with ZnNi alloy in alkaline solution. They found no change in Zn or Ni content in the alloy or in the efficiency of the process when SiC was added to the solution or incorporated into the deposit. However, the crystal size of the deposited ZnNi was reduced. Tulio et al. [5] found, in slightly acid electrodeposition solutions, a smaller Ni/Zn ratio in ZnNi–Al_2O_3 electrocomposites than in ZnNi or ZnNi–SiC films. Takahashi et al. [6] studied the co-deposition of nanosized colloidal SiO_2 particles with ZnFe, ZnCr, ZnNi, and ZnCo alloys from sulfate solutions. They found a synergetic effect between the Fe, Cr, Ni, Co, and SiO_2 contents in the respective alloys. They termed this phenomenon "induced co-deposition".

The alloy composition and electrochemical behavior may be affected by inert particles added to the baths. It is important to understand their influence on alloy composition since, for example, the corrosion resistance [7] depends on it.

The aim of the present study is to contribute to the understanding of the electrodeposition of metal-alloy

P. C. Tulio (✉) · I. A. Carlos
Department of Chemistry, Federal University of São Carlos,
Rodovia Washington Luis km 235, P. O. Box 676,
CEP 13565-905 Sao Carlos, SP, Brazil
e-mail: pctulio@yahoo.com.br

composites. The chosen systems were the electrodeposition of Zn, Co, and ZnCo films from acidic sulfate solutions containing hard particles of SiC or Al_2O_3. ZnCo is an important alloy, especially as it has better corrosion resistance than pure Zn [7]. Incorporation of SiC and Al_2O_3 could improve its tribological properties and enhance its performance.

2 Experimental

The working electrode (WE) was a rotating disk electrode (RDE) consisting of an interchangeable mild steel cylinder embedded in an epoxy resin, with an electroactive flat disk surface area of 0.38 cm^2. Before each experiment, WE was polished with 600-emery paper, rinsed with distilled-deionized water and dried. The counter-electrode was a Pt plate (1 cm^2) and the reference electrode to which all the potentials were referred was a normal calomel electrode (NCE, 1 N KCl). All electrochemical measurements were conducted at room temperature (25 °C) under forced convection conditions produced by the RDE at a constant frequency (ω) of 600 rpm. Current density (i)–potential (E) curves were obtained at a constant sweep rate (v) of 10 mV s^{-1}. Details of the experimental set-up for electrochemical measurements can be found elsewhere [1].

The electrodeposition solutions were: 0.4 M $ZnSO_4 \cdot 7H_2O$ + 0.3 M H_3BO_3 + 1 M NH_4Cl for Zn, 0.4 M $CoSO_4 \cdot 7H_2O$ + 0.3 M H_3BO_3 + 1 M NH_4Cl for Co and 0.4 M $ZnSO_4 \cdot 7H_2O$ + 0.4 M $CoSO_4 \cdot 7H_2O$ + 0.3 M H_3BO_3 + 1 M NH_4Cl for ZnCo films. The pH of each solution was adjusted to 2 with H_2SO_4. All the reagents were of analytical grade and the water was distilled-deionized water (ddw). The electrochemical cell was a cylindrical beaker of 150 cm^3 capacity.

The ceramic particles consisted of, as-received, 97.73% pure α-SiC, mean diameter (ϕ_m) 9.5 μm, and 99.85% pure α-Al_2O_3 (ϕ_m = 3.4 μm), kindly furnished by Treibacher-Schleifmittel Brazil Ltd. Distinct loadings of SiC (C_{SiC}) and Al_2O_3 ($C_{Al_2O_3}$) were added to the electrodeposition solutions. For good dispersion and disaggregation of particles, the solutions were stirred magnetically for at least 12 h before electrochemical experiments. During the electrodeposition, the magnetic stirring was stopped and only the disk rotation was maintained.

Scanning Electron Microscopic (SEM) examination of surface morphology and energy-dispersive x-ray spectroscopy (EDX) semi-quantitative microanalysis of deposit surfaces were performed with a Zeiss Digital Scanning Microscope DSM-960 and an Isis Oxford Instruments Si(Li) Link EDX detector, Serial Number 21869. Films obtained at constant galvanostatic cathodic current densities (i_g) were analyzed. The deposited charge density (q_d) was 80 C cm^{-2}, which, by Faraday's law, corresponds approximately to 33 μm of coating thickness, assuming 100% current efficiency. The freshly obtained deposits were vigorously rinsed with ddw, dried and immersed in an ultrasonic water bath for 15 min. After this, they were vigorously rinsed with water, dried and put in a desiccator. This procedure was performed to remove any SiC or Al_2O_3 loosely adsorbed on the deposit surface. In the EDX analysis, a central area of approximately 3.6 × 2.5 mm^2 was analyzed to determine the mean concentration in a large area. The Si and Al content in the deposits were analyzed and the weight percent (wt%) of SiC and Al_2O_3 in the deposit was obtained from the stoichiometric 1:1 and 2:3 atomic ratios, respectively.

3 Results and discussion

3.1 The effects of SiC and Al_2O_3 on Zn electrodeposition

Figure 1a, b shows the effects of distinct C_{SiC} and $C_{Al_2O_3}$ on the beginning of Zn electrodeposition. In accordance with [1], the peak c_0, in the pre-bulk electrodeposition region, has contributions from Zn upd and the hydrogen evolution reaction from H_3O^+ reduction (HER). In the bulk electrodeposition there is the region c_1, corresponding to a primary nucleation and diffusion-controlled growth and after that, a secondary nucleation and growth causes the current density to increase again. The addition of SiC or Al_2O_3 particles has effects on the current densities of these processes. The pre-bulk electrodeposition of Zn is not affected by SiC but with Al_2O_3, higher current densities are attained. With SiC, there is practically no change in the initial potential for Zn bulk deposition. On the other hand, with Al_2O_3, a small polarization is observed with higher initial current densities as $C_{Al_2O_3}$ increases.

For Zn bulk electrodeposition, both, SiC and Al_2O_3 increase the current densities in the cathodic sweep up to E_λ (switching potential) relative to the particle-free curves. Also, the higher current densities observed in the anodic branches of Fig. 1 for SiC or Al_2O_3 indicate that the higher cathodic current densities are related to Zn electrodeposition and not to the HER, as may be verified by the high anodic to cathodic charge density ratios ($|q_a/q_c|$) shown in Fig. 2. The q_c was estimated only for the bulk electrodeposition. For Al_2O_3, there is a maximum in the $|q_a/q_c|$ ratio which may be due to the aggregation of Al_2O_3 at the bottom of the cell at high $C_{Al_2O_3}$ during electrodeposition, making the effective concentration of Al_2O_3 smaller.

Both, SiC and Al_2O_3 particles increased the Zn electrodeposition rate. A visual inspection of the electrode surface, after a cathodic sweep up to E_λ of −1.19 V in the

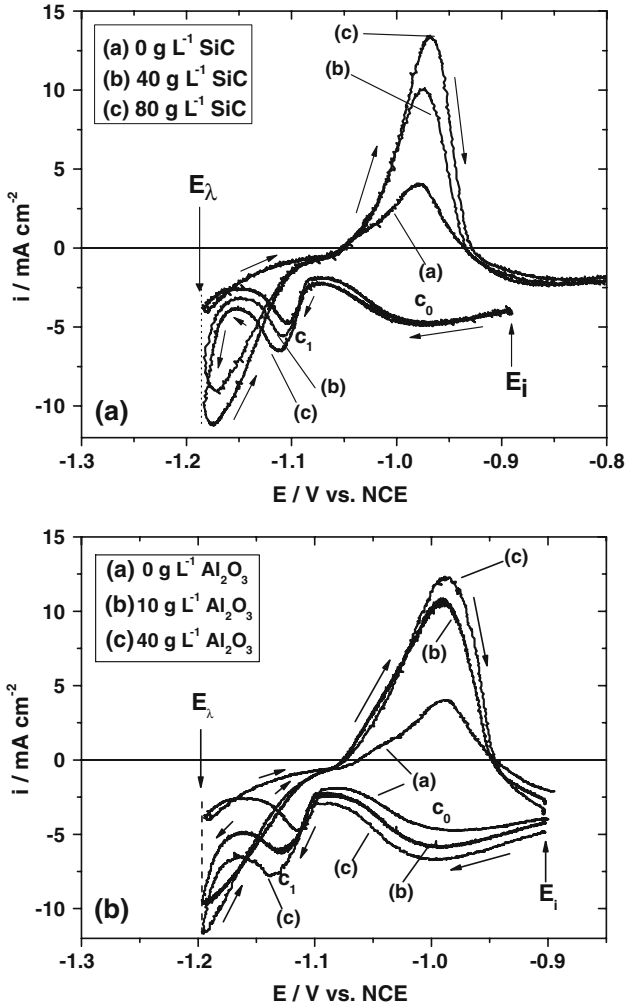

Fig. 1 **a** Typical i–E curves for the steel electrode in the Zn electrodeposition solution (0.4 M $ZnSO_4 \cdot 7H_2O$ + 0.3 M H_3BO_3 + 1 M NH_4Cl) loaded with various C_{SiC}, as indicated; **b** the same as (**a**) for various C_{Al2O3}. $\omega = 600$ rpm, $v = 10$ mV s^{-1}. E_i = Starting potential. E_λ = Switching potential

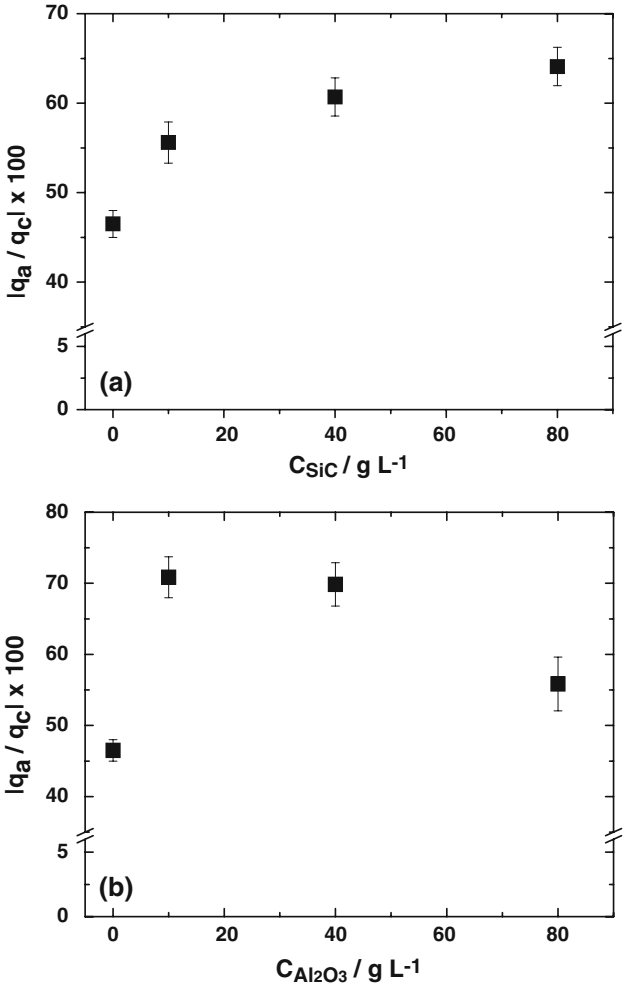

Fig. 2 **a** The dependence of the $|q_a/q_c|$ ratio on C_{SiC} for voltammetric zinc electrodeposition curves like those in Fig. 1a. **b** The dependence of the $|q_a/q_c|$ ratio on $C_{Al_2O_3}$ for voltammetric curves like those in Fig. 1b

solution with SiC or Al_2O_3, shows that a much higher quantity of Zn covers the electrode surface. The higher the C_{SiC} or $C_{Al_2O_3}$, the higher is the quantity of electrodeposited Zn. These results suggest that SiC or Al_2O_3 do not block the active sites on the electrode surface for Zn electrodeposition. Rather, they promote Zn electrodeposition over the steel surface.

Many authors have observed similar effects of inert particles on cathodic sweeps and several hypotheses have been proposed to explain the results. Examples are: increase in electroactive electrode area due to particles adsorbed on it [8, 9]; changes in texture promoted by the particles [10]; migration component [8], and turbulent flow promoted by the particles [11]. Other systems, in contrast, exhibit polarization and this is attributed to ohmic drop in the solution [12] or surface blockage of the electrode caused by the particles [2, 10].

In this study, the larger current densities obtained when Al_2O_3 or SiC particles were added to the Zn electrodeposition solution cannot be attributed to migration, in view of the high ionic concentration of the solutions and the large size of the particles. Grosjean et al. [13] obtained an ionic mobility of zero for SiC when working with 10^{-1} M $NiSO_4$ or $NiCl_2$ solutions. The electroactive surface area might be increased, but not by adsorbed particles as this would cause polarization. Turbulent flow, as pointed out by Lee and Choi [11], could be a plausible hypothesis, for the micro-sized SiC ($\phi_m = 9.5$ μm) and Al_2O_3 (3.4 μm) used in this work.

To explain the action of SiC and Al_2O_3 shown in Figs. 1 and 2, features of the Zn electrodeposition processes [1] must be considered. In region c_1 there is a primary nucleation and diffusion-controlled growth [1]. The diffusion layers are formed around the growing nuclei, generating exclusion zones. These hinder the formation of new nuclei

on active sites within these zones, giving rise to the low degrees of coverage of the steel surface by Zn under forced convection. Also, there will be hindering of the secondary nucleation and growth. It must be emphasized that the SiC and Al_2O_3 particles have mean diameters which are of the order of the thickness of the Nernst diffusion layer under forced convection conditions (10 μm) [14]. As the electrode rotation rate causes the particles to impinge against the electrode surface, this movement drags fresh solution, together with the impinging particles, on to the electrode surface, thus increasing solution mass-transport. This disturbs the exclusion zone development around the Zn nuclei formed in region c_1 [1], allowing new nucleation and growth, with higher current densities in c_1 and higher quantities of Zn electrodeposited. As a result, secondary nucleation and growth will also be favored, as observed, explaining the larger quantities deposited. This must be the basic reason for the effects observed in Fig. 1. In light of this effect, SiC and Al_2O_3 may be thought of as additives that promote Zn electrodeposition from acidic solutions.

3.2 The effects of SiC and Al_2O_3 micro particles on Co electrodeposition

In contrast to the electrodeposition of zinc, that of cobalt is affected differently by SiC and Al_2O_3 as can be seen in Fig. 3. The addition of SiC (Fig. 3a) has effects on the i–E curves similar to those for Zn electrodeposition (Fig. 1a). As C_{SiC} increases, so do the current densities for the processes occurring at potentials more negative than −0.85 V in the i–E curve for Co electrodeposition, especially at high C_{SiC}. An increase in the solution mass-transport, caused by the impinging of microsized SiC particles on the electrode surface, leads to an increase in the number of Co nuclei on the steel substrate, promoting Co electrodeposition.

Particles of Al_2O_3, on the other hand, have a negative effect on Co electrodeposition, mainly for the first process, c_{Co1} (Fig. 3b). It can be assumed that a complex mechanism is acting in the Co–Al_2O_3 electrodeposition system since, for Zn electrodeposition, under the same conditions, the current density increases with $C_{Al_2O_3}$ for all the processes (Fig. 1b). Blockage of the electrode surface by positively charged Al_2O_3 at pH = 2 [15], cannot be responsible, since the same would occur for Zn electrodeposition (Fig. 1b), which is clearly not the case.

Wu et al. [3], studying CoNi electrodeposition from sulfamate electrolytes (pH = 4) at high $[Co^{2+}/Ni^{2+}]$ ratios in solution, found a strong tendency of Co^{2+} to adsorb on α-Al_2O_3 (ϕ_m = 0.5 μm) in that medium. The authors argued that this promotes both Co enrichment and Al_2O_3 co-deposition in the CoNi electrodeposited matrix. Smaller current densities in Fig. 3b could be related to a decrease in the Co^{2+} concentration at the electrode surface. One possibility is that the Co^{2+} ions could be adsorbed on the Al_2O_3 surface as Wu et al. [2, 3] observed, reducing $[Co^{2+}]$ or hindering its reduction. What is clear is that the Al_2O_3 particles used here have had negative effects on Co electrodeposition and this may be related to the difficulties in the deposition of Co from Al_2O_3-containing ZnCo electrodeposition solutions, as will be seen in Sect. 3.4.2.

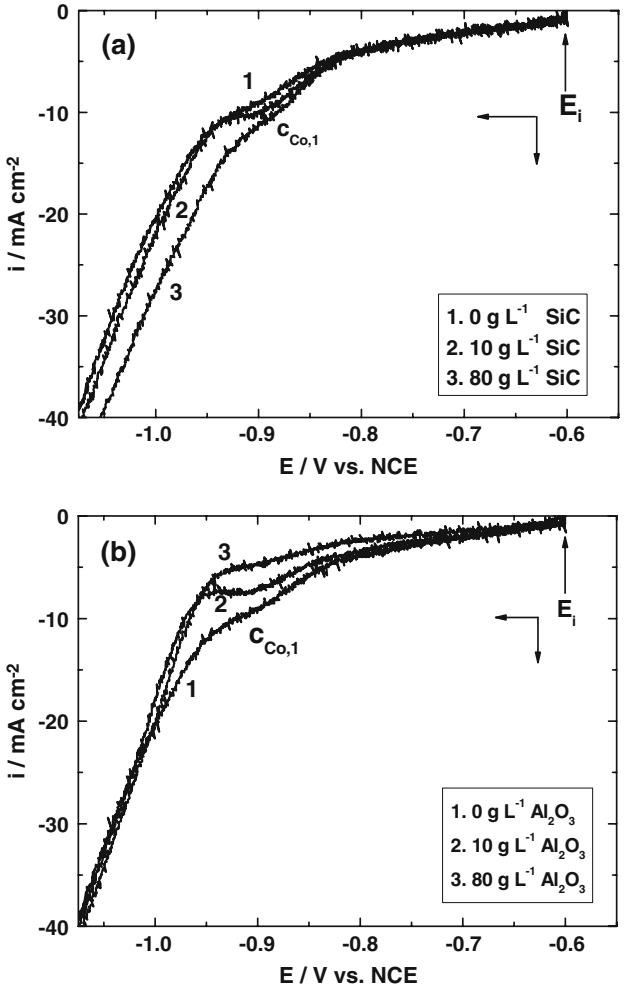

Fig. 3 Typical i–E curves for the steel electrode in the cobalt electrodeposition solution (0.4 M $CoSO_4 \cdot 7H_2O$ + 0.3 M H_3BO_3 + 1 M NH_4Cl) loaded with various C_{SiC} (**a**) and $C_{Al_2O_3}$ (**b**), as indicated. ω = 600 rpm, ν = 10 mV s^{-1}. E_i = Starting potential

3.3 Effects of SiC and Al_2O_3 micro particles on ZnCo electrodeposition

The effects of SiC and Al_2O_3 particles on ZnCo electrodeposition can be analyzed in Fig. 4. With SiC, the current densities in the first process c_1 are higher than in the particle-free solution, but they are practically insensitive to C_{SiC}. After c_1, for all C_{SiC}, current densities are higher than in the particle-free solution, due to the increased solution mass-transport promoted by the SiC particles. However, at C_{SiC} of

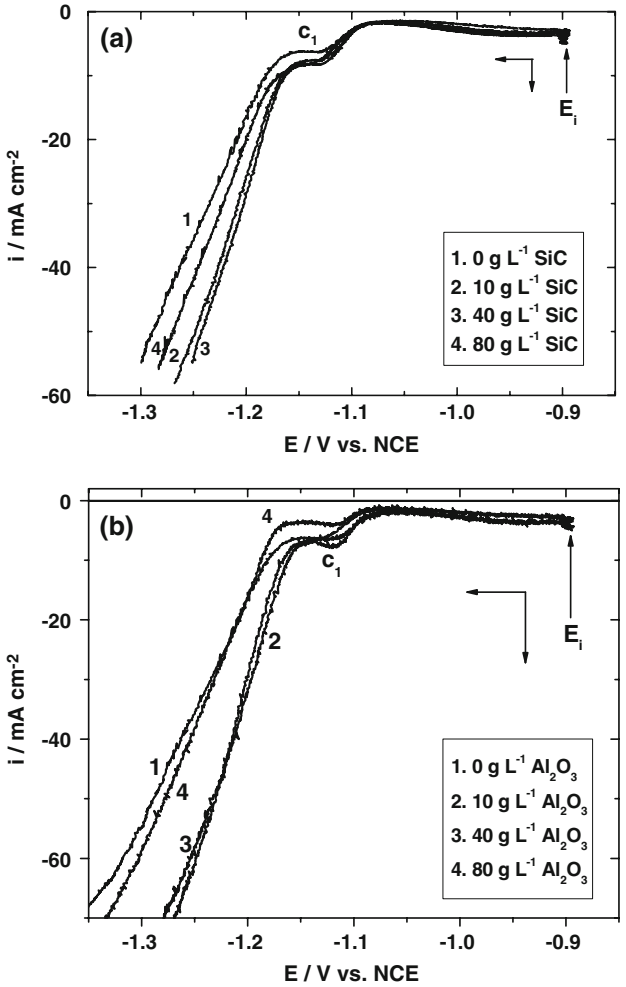

Fig. 4 Typical i-E curves for the steel electrode in the zinc–cobalt electrodeposition solution (0.4 M $ZnSO_4 \cdot 7H_2O$ + 0.4 M $CoSO_4 \cdot 7H_2O$ + 0.3 M H_3BO_3 + 1 M NH_4Cl) loaded with various C_{SiC} (**a**) and $C_{Al_2O_3}$ (**b**), as indicated. $\omega = 600$ rpm, $v = 10$ mV s^{-1}. E_i = Starting potential

80 g L^{-1} the current densities are lower than C_{SiC} of 10 and 40 g L^{-1}, probably due to blocking of the electrode surface by SiC particles at more negative potentials.

The i–E curves for ZnCo electrodeposition in the presence of Al_2O_3 have practically the same features as those for SiC. Here the differences are seen in the region c_1, where practically no effects are seen at C_{Al2O3} of 10 and 40 g L^{-1}, while the blocking effect at 80 g L^{-1} Al_2O_3 is already present at c_1.

3.4 Compositional analysis of ZnCo–SiC and ZnCo–Al_2O_3 composites

ZnCo–SiC and ZnCo–Al_2O_3 composites were prepared. Analysis was carried out on galvanostatically obtained composites with q_d of 80 C cm^{-2} at a fixed ω of 600 rpm and for a fixed C_{SiC} and $C_{Al_2O_3}$ of 40 g L^{-1}.

3.4.1 Analysis of ZnCo–SiC

A scanning electron micrograph of a transverse section of a ZnCo–SiC electrocomposite is shown in Fig. 5. Some occluded SiC particles can be seen. In Fig. 6, the variation of the SiC content in these composites is plotted against i_g. Taking the error bars into account, it is seen that SiC content is practically independent of i_g.

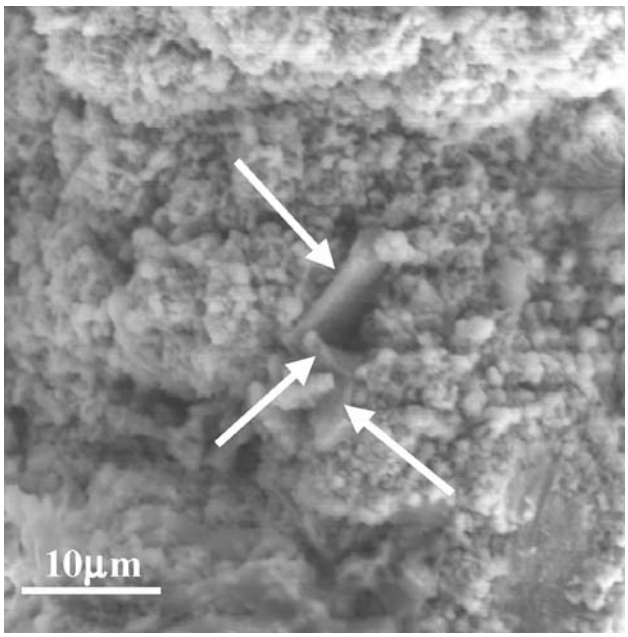

Fig. 5 SEM photograph of a transverse section of a ZnCo–SiC electrocomposite film in which some occluded SiC particles are indicated by arrows

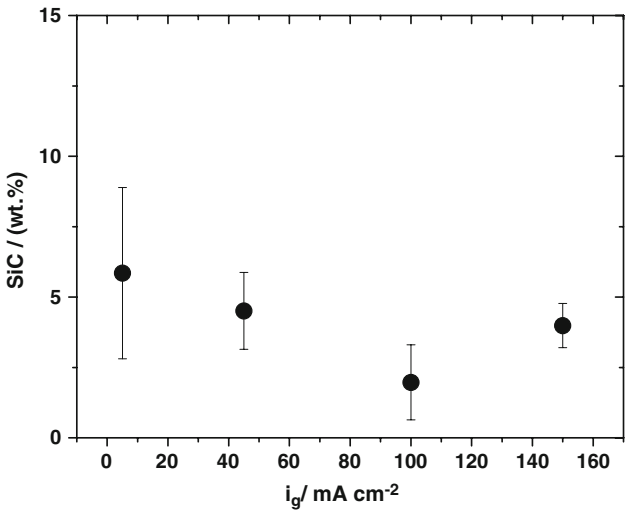

Fig. 6 Variation in the SiC content as a function of i_g in 80 C cm^{-2} ZnCo–SiC electrocomposites deposited at 600 rpm from ZnCo electrodeposition solution loaded with 40 g L^{-1} of SiC

The Co content of the ZnCo deposits, analyzed by EDX, was low, varying between 0.3 and 0.6 wt%. Nevertheless, this composition is of interest for the purpose of corrosion protection [7]. The Co content was a function of i_g and of the presence of SiC in the electrodeposition solution, as seen in Fig. 7, in the variation of the [Co(wt%)/Zn(wt%)] ratio. The error bars in Fig. 7 are large because of the low Co content. In spite of this, it is clear that Co content in the deposit increased when SiC was added to the ZnCo solution, especially for $i_g > 5$ mA cm^{-2}. The ZnCo anomalous deposition is not eliminated by SiC, but it is attenuated to a small extent when SiC is present in the ZnCo solution. EDX microanalysis at points around occluded SiC particles did not show significant deviations in the [Co(wt%)/Zn(wt%)] ratios from those shown in Fig. 7. This shows the higher percentages of Co in the ZnCo–SiC films are not related to the occlusion mechanism of SiC.

The results can be correlated with the individual effects of SiC particles on Zn and Co electrodeposition curves shown in Figs. 1a and 3a, respectively. In both cases, SiC particles enhance the electrodeposition rates. Based on this, the results in Fig. 7 may be interpreted as a promotion of the Co^{2+} reduction when both Co^{2+} and Zn^{2+} are in the solution loaded with SiC particles. For this interpretation to be valid it must be assumed that the individual behavior of the i–E curves for separate Zn and Co electrodeposition seen in Figs. 1a and 3a is maintained during ZnCo electrodeposition. This may be a rough approximation. Additional experiments are necessary to reach conclusive explanations. However, the results in Fig. 7 are important since, in these ZnCo–SiC composite coatings, SiC particles can change the metal matrix composition and, consequently, some properties, such as, the corrosion resistance.

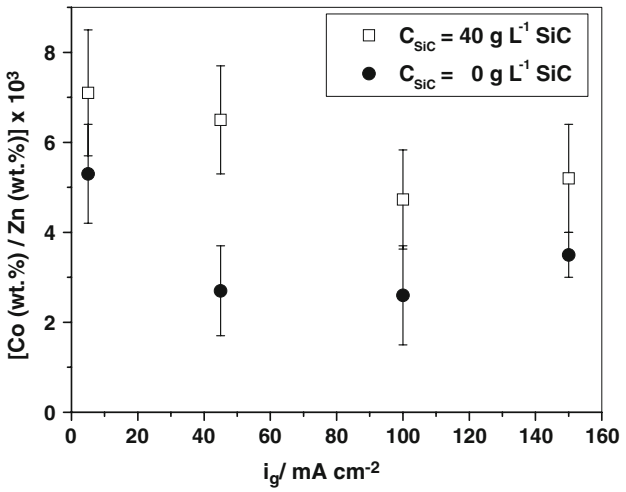

Fig. 7 Variation of [Co(wt%)/Zn(wt%)] ratio, as a function of galvanostatic current density (i_g) in 80 C cm^{-2} ZnCo and ZnCo–SiC electrocomposites deposited from particle-free and from 40 g L^{-1} SiC-loaded ZnCo electrodeposition solutions, respectively, as indicated in the figure. $\omega = 600$ rpm

3.4.2 *Analysis of ZnCo–Al_2O_3*

In this case, features distinct from those of ZnCo–SiC composites were observed. The first is that for the solution containing 0.4 M $CoSO_4$, the Co content in the films was below the EDX threshold. However, it is assumed that Co is present. The same was observed for the co-deposited Al_2O_3, except at an i_g of 5 mA cm^{-2}, where 3.1 wt% of Al_2O_3 was detected. ZnCo–Al_2O_3 was obtained but, compared to the particle-free and the SiC-loaded electrodeposition solutions, there is now a mutual hindering of Co^{2+} reduction and Al_2O_3 incorporation, the anomalous electrodeposition being accentuated.

Regarding the difficulties in Al_2O_3 incorporation, a second observed feature was that in ZnCo electrodeposition solutions containing 0.1 M $CoSO_4$, Al_2O_3 was detected in the films by EDX analysis over the whole analyzed i_g range (the same range as for ZnCo–SiC), which was not the case for 0.4 M $CoSO_4$. The Al_2O_3 particle content did not exceed 3.5 wt%. Co was not detected since it remained below the EDX threshold, but it was assumed to be present. These observations may indicate that Al_2O_3 incorporation into the metal matrix depends on the Co^{2+} concentration in solution and on the growth rate of the deposits. These difficulties must be overcome when obtaining ZnCo–Al_2O_3 electrocomposites under the conditions analyzed here.

As in the case of ZnCo–SiC, these results for ZnCo–Al_2O_3 could be correlated with the effects of Al_2O_3 on the individual i–E curves for Zn (Fig. 1b) and Co (Fig. 3b) electrodeposition. A strong enhancement of the Zn electrodeposition rate and a negative effect on Co electrodeposition were seen when Al_2O_3 particles were added to the respective solutions. Even with the approximation of supposing that these individual effects are present in the ZnCo electrodeposition, there is some coherence between the results which explains the increase in Zn content relative to Co in the ZnCo matrix. However, additional experiments are necessary to clarify these effects, since they may also be related to adsorption of Zn^{2+} or Co^{2+} onto the Al_2O_3 particles. For example, Wu et al. [2, 3], in a CoNi–Al_2O_3 system, found an increase in the Co content of the metallic matrix. They assumed that strong adsorption of Co^{2+} on the Al_2O_3 surface promoted increases in both Co and Al_2O_3 contents in the CoNi matrix.

For the ZnCo deposits analyzed, what is clear is that as [Co^{2+}] is increased, it hinders Al_2O_3 co-deposition and Al_2O_3 hinders Co^{2+} reduction, at least in more concentrated Co^{2+} solutions.

4 Conclusions

The addition of SiC or Al_2O_3 microsized particles to an acid sulfate zinc electrodeposition solution substantially enhanced the rate of Zn initial electrodeposition, compared to that from particle-free solution.

The addition of SiC to an acid sulfate solution for cobalt deposition increased the current densities for Co deposition i–E curves, thus promoting electrodeposition. On the other hand, addition of Al_2O_3 had a hindering effect on Co deposition. Current densities were decreased when Al_2O_3 particles were added to the solution, especially at the beginning of i–E curves.

For ZnCo electrodeposition it was found that the addition of SiC or Al_2O_3 particles to the solution affected the i–E curves, increasing the current densities especially far from the initial deposition potentials and at moderate C_{SiC} and $C_{Al_2O_3}$.

ZnCo–SiC composites were obtained over the whole studied range of galvanostatic current densities (i_g). The SiC content was practically independent of i_g. With SiC in the solution, higher [Co/Zn] ratios were obtained in the metal matrix compared to the ZnCo films from particle-free solutions.

For ZnCo–Al_2O_3 composites, it was observed that when Al_2O_3 was added to the solution, the Co^{2+} reduction was hindered and it was hard to co-deposit the Al_2O_3. In order to obtain co-deposition of Al_2O_3 it was necessary to reduce the $CoSO_4$ concentration.

The results for the ZnCo film composition of the composites could, in principle, be related to the effects of SiC and Al_2O_3 on the individual curves for Zn and Co deposition. SiC promoted both Zn and Co deposition. Al_2O_3 strongly promoted Zn electrodeposition and had a negative effect on Co electrodeposition.

Acknowledgments P. C. Tulio is grateful to Fundação de Amparo à Pesquisa do Estado de São Paulo (FAPESP) for his Ph. D. grant. The authors are grateful to Treibacher-Schleifmittel Brazil Ltd. which kindly furnished the SiC and Al_2O_3 used in this work.

References

1. Tulio PC, Carlos IA (2009) J Appl Electrochem 39:283. doi: 10.1007/s10800-008-9670-8
2. Wu G, Li N, Zhou D et al (2004) Surf Coat Technol 176:157
3. Wu G, Li N, Wang DL et al (2004) Mat Chem Phys 87:411
4. Muller C, Sarret M, Benballa M (2002) Surf Coat Technol 162:49
5. Tulio PC, Rodrigues SEB, Carlos IA (2007) Surf Coat Technol 202:91
6. Takahashi A, Miyoshi Y, Hada T (1994) J Electrochem Soc 141:954
7. Wilcox GD, Gabe DR (1993) Corr Sci 35:1251
8. Benea L, Bonora PL, Borello A, Martelli S et al (2001) J Electrochem Soc 148:C461
9. Watson SW (1993) J Electrochem Soc 140:2235
10. Socha RP, Nowak P, Laajalehto K et al (2004) Colloids Surf A 235:45
11. Lee EC, Choi JW (2001) Surf Coat Technol 148:234
12. Nowak P, Socha RP, Kaisheva M et al (2000) J Appl Electrochem 30:429
13. Grosjean A, Rezrazi M, Tachez M (1997) Surf Coat Technol 96:300
14. Hamann CH, Hamnett A, Vielstich W (1998) Electrochemistry. Wiley-VCH, New York
15. Brinker CJ, Scherer GW (1990) Sol–gel science: the physics and chemistry of sol–gel processing. Academic Press, New York